Factors affecting the growth of multi-seeded superconducting single grains

Yunhua Shi, Anthony R Dennis, Difan Zhou, Devendra K Namburi, Kaiyuan Huang, John H Durrell and David A Cardwell*

Department of Engineering, University of Cambridge, Trumpington Street, Cambridge, CB2 1PZ, UK

Abstract

Single grain, rare earth–barium–copper oxide [(RE)BCO] bulk superconductors, fabricated either individually or assembled in large or complicated geometries, have significant potential for a variety of potential engineering applications. Unfortunately, (RE)BCO single grains have intrinsically very low growth rates, which limits the sample size that may be achieved in a practical, top seeded melt growth (TSMG) process. As a result, a melt process based on the use of two or more seeds (so-called multi-seeding) to control the nucleation and subsequent growth of bulk (RE)BCO superconductors has been developed to fabricate larger samples and to reduce the time taken for the melt process. However, the formation of regions that contain non-superconducting phases at grain boundaries has emerged as an unavoidable consequence of this process. This leads to the multi-seeded sample behaving as if it is composed of multiple, singly seeded regions. In this work we have examined the factors that lead to the accumulation of non-superconducting phases at grain boundaries in multi-seeded (RE)BCO bulk samples. We have studied the microstructure and superconducting properties of a number of samples fabricated by the multi seeded process to explore how the severity of this problem can be reduced significantly, if not eliminated completely. We conclude that, by employing the techniques described, multi-seeding is a practical approach to the processing of large high performance superconducting bulk samples for engineering applications.

Yunhua Shi
Department of Engineering,
University of Cambridge, Trumpington Street,
Cambridge, CB2 1PZ, UK
Tel: +44 1223 32831
Email: ys206@cam.ac.uk

Factors affecting the growth of multi-seeded superconducting single grains

Yunhua Shi*, Anthony R Dennis, Difan Zhou, Devendra K Namburi, Kaiyuan Huang, John H Durrell and David A Cardwell

Abstract

Single grain, rare earth–barium–copper oxide [(RE)BCO] bulk superconductors, fabricated either individually or assembled in large or complicated geometries, have significant potential for a variety of potential engineering applications. Unfortunately, (RE)BCO single grains have intrinsically very low growth rates, which limits the sample size that may be achieved in a practical, top seeded melt growth (TSMG) process. As a result, a melt process based on the use of two or more seeds (so-called multi-seeding) to control the nucleation and subsequent growth of bulk (RE)BCO superconductors has been developed to fabricate larger samples and to reduce the time taken for the melt process. However, the formation of regions that contain non-superconducting phases at grain boundaries has emerged as an unavoidable consequence of this process. This leads to the multi-seeded sample behaving as if it is composed of multiple, singly seeded regions. In this work we have examined the factors that lead to the accumulation of non-superconducting phases at grain boundaries in multi-seeded (RE)BCO bulk samples. We have studied the microstructure and superconducting properties of a number of samples fabricated by the multi seeded process to explore how the severity of this problem can be reduced significantly, if not eliminated completely. We conclude that, by employing the techniques described, multi-seeding is a practical approach to the processing of large high performance superconducting bulk samples for engineering applications.

Key Words

Multi-seeding, Grain boundaries, Alignment, Buffer, Quasi-single grains, Practical, YBCO, GdBCO-Ag

1 INTRODUCTION

Single grain, rare earth–barium–copper oxide [(RE)BCO] bulk superconductors assembled in large and/or complicated geometries are required for a variety of potential engineering applications, such as energy storage flywheels, bearings and levitation platforms [1, 2]. This originates from the ability of these materials to provide self-stabilised levitation and to trap

much larger magnetic fields than those that can be generated using conventional permanent magnets. Indeed, a stack of two GdBCO-Ag single grain samples of diameter 25 mm has been shown relatively recently to generate a trapped field of 17.6 T at 26 K [3]. However, the growth of individual (RE)BCO single grains is a rather complex and slow process based on top seeded melt growth (TSMG). Samples of only 25 mm in diameter, for example, require five days to grow due to the narrow growth window of approximately 30°C in the TSMG process and a growth rate that is limited, typically, to 0.5 mm/hour [4, 5]. Multi-seeding, where sample growth is initiated from multiple, aligned, seeds rather than from a single seed, offers the prospect of faster sample growth and, therefore, the fabrication of larger samples for practical processing times.

(RE)BCO bulk superconductors grown from a seed crystal are best described as constituting single grains, rather than single crystals. The matrix of the single grain is comprised mainly of fully connected $REBa_2Cu_3O_{7-\delta}$ (RE-123, where, typically, $\delta \leq 0.5$) with numerous, embedded discrete RE_2BaCuO_5 (RE-211) inclusions. The embedded RE-211 phase has the important property of acting as effective flux pinning centres, which improves the superconducting critical current of the single grain [6][[7]. Good quality single grains fabricated with one seed typically exhibit four characteristic facet lines on the top surface of the sample, as shown in figure 1(a). Importantly, these facet lines are not grain boundaries, but indicate the positions at which the crystallographic growth fronts impinge (similar features are evident in the growth morphology of single crystal silicon). A typical trapped field profile in a bulk single grain superconductor, generated by induced, persistent supercurrents, is of conical geometry with a slope determined by the size of the critical current density, J_c. A typical cross section and a 2D field profile for a single grain fabricated by TSMG sample are shown in figures 1(b) and (c). The uniformity of the trapped field profile and the height of the peak field value indicate the quality of the sample, at least in terms of the properties required for practical applications.

The primary advantage of multi-seeding is the ability to fabricate large and complex superconducting bulk materials and structures without increasing processing time. However, this process also introduces the complication of the formation of grain boundaries where two growth fronts meet, as shown in figure 1(d) [8-16]. Consequently, the resulting trapped field profile generally exhibits two, deeply split peaks with lower peak field values, as shown in figures 1(e) and (f), indicating that there is no significant flow of super-current through the

grain boundary, which reduces trapped field accordingly. The reduction in critical current at these zero angle grain boundaries, however, is not due to the effects of misorientation, as observed in other systems, such as thin films and coated conductors [17]. Studies of microstructure and composition of these grain boundaries indicate that there exist CuO rich non-superconducting phases at the grain boundary region and that the thickness of an individual boundary can be as large as 50 μm [16]. Therefore, the question arises whether it is possible or effectively practical to fabricate multi-seeded single grains.

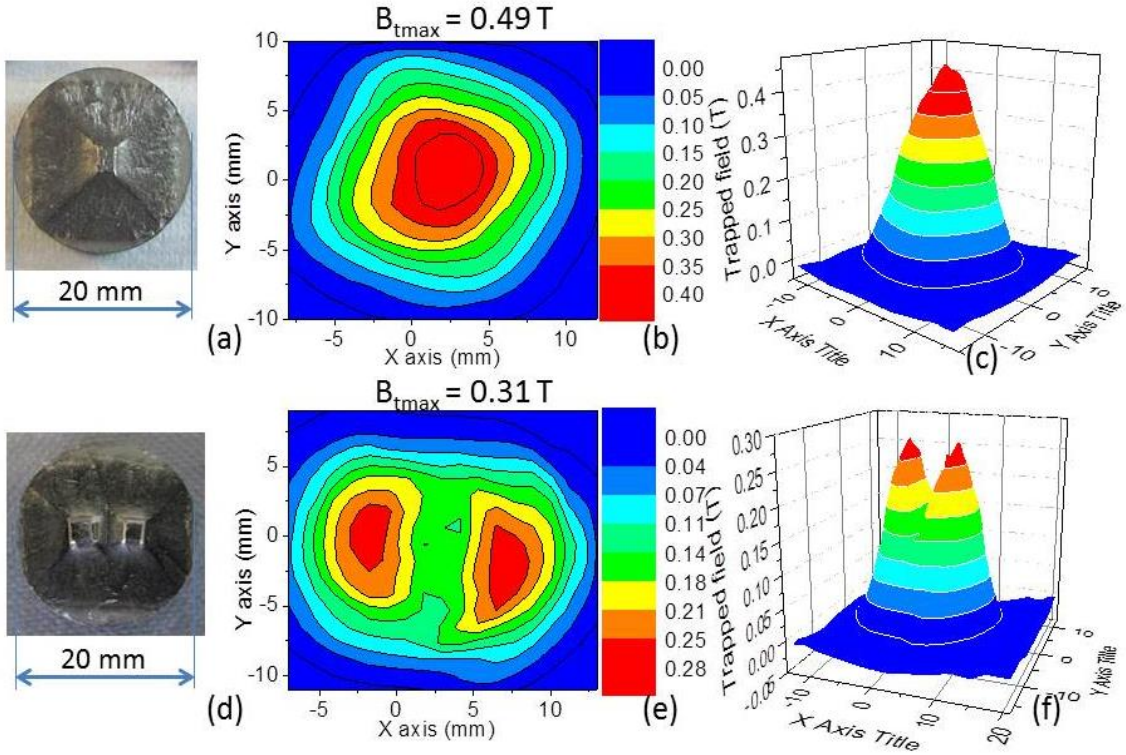

Figure 1. Bulk superconducting samples and their trapped field profiles (a) A photograph of a YBCO single grain, (b) a contour map of the trapped field measured at 77 K of the sample in (a), (c) trapped field profile at 77 K of the sample in (a), (d) a photograph of a multi- seeded YBCO bulk sample, (e) a contour map of the trapped field at 77K of the sample in (d) and (f) trapped field profile at 77 K of the sample in (d).

In this paper we address systematically, within the context of previous work [8-11, 13, 18-23], the factors that affect the growth of multi-seeded, bulk superconducting grains. These include the distance between seeds, the seed and buffer layer combination and seed alignment. We demonstrate that it is possible to fabricate multi-seeded bulk (RE)BCO superconductors that exhibit properties that approach those of a single grain with careful control of the distance,

size and alignment of the seeds. These multi-seeded samples, therefore, effectively constitute quasi-single grains.

2 EXPERIMENTAL PROCEDURES

Six melt processed samples grown using various numbers of seeds and seed orientations for both YBCO and GdBCO-Ag samples were investigated as part of this study. The compositions of the precursor powder for these samples were (75wt% Y-123 +25wt% Y-211) + 0.5wt% CeO_2 and (75wt%Gd-123 + 25wt% Gd-211) + 1wt% BaO_2 + 0.1wt% Pt + 10wt% Ag_2O, respectively, with the main RE-123 and RE- 211 precursors (99.9% purity) supplied by Toshima Ltd., Japan. The mixed precursor powders were pressed uniaxially into the required dimensions and seeds were placed on the top surfaces of each pressed sample before it was loaded into a box furnace for melt-processing in air using a conventional TSMG heating profile, as shown in figure 2. Table 1 summarises the main parameters of the as melt-processed grains. The successfully grown samples were subsequently annealed in pure oxygen (99.9%) at a temperature in the range 450 °C to 400 °C for 10 days to allow the lattice structure of the sample to change from the non-superconducting tetragonal to the superconducting orthorhombic phase.

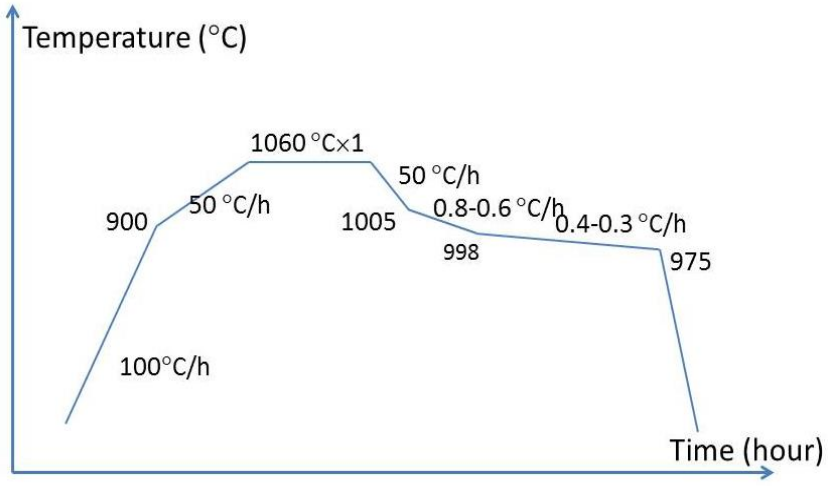

Figure 2. Heating profiles used to melt-process YBCO and GdBCO-Ag single grains.

Table 1. The main parameters of samples 1 to 6

Sample	Type	Dimensions post processing (mm)	Weight (g)	Seeds	Photographs of the samples
1	YBCO	60×20×12 (L×W×H)	78	Two SmBCO 45°-45° bridge seeds	
2	YBCO	60×20×12 (L×W×H)	78	Two SmBCO 0°-0° bridge seeds	
3	YBCO	31×13 Ø × R	65	Two SmBCO 45°-45° bridge seeds	
4	YBCO	60×20×14 (L×W×H)	85	Three SmBCO seeds with buffers aligned 0°-0°-0°	
5	YBCO	25×12 Ø × R	46	2 SmBCO seeds with buffers aligned 0°-0°	
6	GdBCO-Ag	20×10 Ø × R	20	NdBCO (on MgO) film seeds [24]	

The trapped field of each sample was measured at 77 K in order to investigate the extent to which the grain boundaries affect the quality of the multi-seeded superconducting grains. Samples 1 to 5 were magnetised by a Field-Cooled (FC) process in an applied field of 1.4 T and the trapped fields measured by an array of 18 rotating Hall probes driven by a stepper motor. The positions of the probes are at approximately between 1.0 and 1.5 mm above the top surface of the sample. The maximum trapped field value of a sample was measured by a handheld Hall probe. The probe rests against the sample surface and its sensor is set back 0.5 mm enabling measurements to be made 0.5 mm above the top surface of each sample.

The top surface of sample 5 was polished repeatedly perpendicular to the c-axis, across the diameter of the cylinder, to reduce its height systematically, with the trapped field measured at each stage to observe the effect of the depth of the grain boundary on the trapped field of the multi-seeded sample. Samples 5 and 6 were also Pulse-Magnetised at 77 K and the

trapped fields at different applied fields recorded by a hand probe at the top surfaces of the samples along the *a* direction in order to improve the accuracy of the measurements. Finally, an additional measurement of trapped field was performed at the bottom of sample 6 in order to observe whether the bottom of the multi-seeded sample actually constituted a single grain.

3 Results and discussion

3.1Major factors that affect the growth of multi-seeded, quasi single grains

Bulk superconducting (RE)BCO single grains consist typically of a continuous superconducting matrix of the orthorhombic $REBa_2Cu_3O_{6.5+\delta}$ ($\delta < 0.5$) (RE-123) phase that contains embedded, non-superconducting $(RE)_2BaCuO_5$ (Y-211) phase inclusions. The four characteristic facet lines that appear on the top surface of a single grain and extend down the side of the grain towards the base of the sample are an immediate visual indication of the formation of a single grain, as shown in figure 3(a). Schematic illustrations of the cross-sections of a single grain seeded in different ways are shown in figure 3(b). The boundaries of the growth sectors, which can usually be seen by eye on a polished cross-section of the sample, are indicated by the dark blue, dashed lines in this figure. The grain boundaries in the multi-seeded samples are highlighted by white, solid lines from the body of the sample towards the seeded surface [samples 2, 3 and 4 in figure 3(b)]. It is known that a grain boundary inevitably forms between two seeds in a multi-seeded sample due to an accumulation of non-superconducting phases (such as RE-211 or solidified Ba-Cu-O liquid phase) [11, 16] where the *a*-sector growth fronts meet and, consequently, limit the flow of supercurrent across this type of grain boundary, even if the seeds are relatively well aligned.

If we assume that grain boundaries are the only sites in a multi-seeded grain where the flow of supercurrent is prohibited, then a sample with a cross-section similar to that indicated by the red dashed line in figure 3(c) should effectively constitute a single grain. In this case, supercurrent can flow within the *ab* planes of the sample, which are usually parallel to the top and bottom surfaces, apart from the "trough" region at the top centre of the sample where two smaller current loops will exist. The profile of trapped field B_t in single grain bulk superconductors is represented typically by a shape that appears very similar to that of a perfect cone if the sample consists of a cylindrical single grain with a flat upper surface. It is easy to understand that the shallower the grain boundary, the higher the trapped field and the closer multi-seeded samples are to single grains (i.e. they form quasi-single grains). In addition, the trapped field profile of such a quasi-single grain would change from two

discreet peaks associated with two, largely independent current loops to having one single peak.

The factors that affect theoretically the depth of the grain boundary are the distance between the seeds [samples 2, 3 and 4 in figure 3(b)] and the alignment and size of the seeds and buffer layer when a buffer is used as an intermediary structure between the seed and the bulk sample [25-28] to aid the seeding process. The slope of the growth sector boundaries (blue dashed line) is also important in determining grain boundary depth (white lines). However, the slope of the *a*-sector boundary (given by θ) is determined by the relative growth rates of the sample in the *a* (or *b*) and *c* directions, which, in turn, depends on the precursor powder, temperature distribution within the furnace and other processing parameters. Although these factors are complicated and might influence one another, they were fixed in the present work in order to minimise their influence.

It is clear from the above discussion that the closer the seeds then the shorter the grain boundary. However, arranging the seeds in close proximity in the multi-seeding process (such as 2 mm apart) is not a desirable approach, either, since this is both challenging and time consuming if good alignment across many seeds is to be achieved. Based on our previous studies [14-16] and the sample geometries developed to date for both research and applications, samples in the range of 20 mm to 60 mm, with an inter-seed distance varying between 6 and 20 mm were fabricated as part of this investigation.

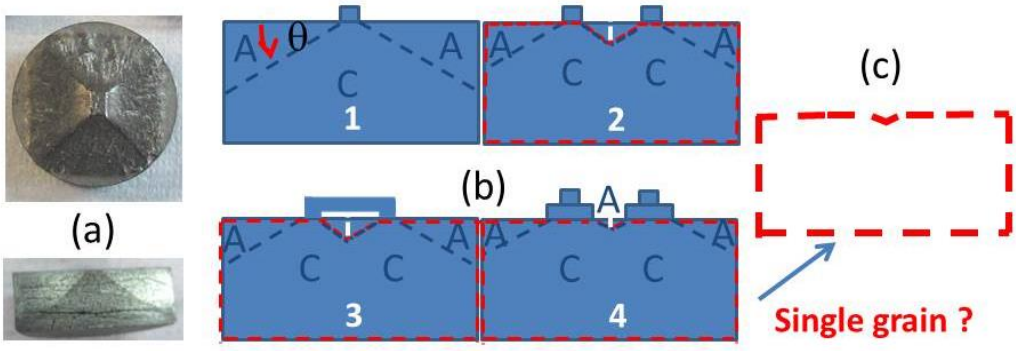

Figure 3. (a) A photograph of a YBCO single grain, (b) schematic representations of the cross-sections of different multi-seeded grains and (c) the shape of the cross-section of a single grain in multi-seeded sample.

3.2 Effect of distance between seeds

Figures 4 (a) and (b) show two, bar-shaped, multi-seeded YBCO grains. Sample 1 was seeded by two, 11 mm long (measured edge to edge) SmBCO 45°-45° bridge seeds [15] and sample 2 was seeded by two, 11 mm long SmBCO 0°-0° bridge seeds [14]. The 2D trapped field contour maps and three dimensional field profiles for samples 1 and 2 are shown in figures 4(c) and (d) and 4(e) and (f), respectively. It can be seen that multiple peaks are present in both samples, suggesting that there are significant grain boundaries between any two adjacent seeds, as discussed previously. It can be deduced for samples 1 and 2 that the depth of the grain boundaries increases with increasing distance between the seeds, as evidenced by the lower trapped field values at positions where the distance between adjacent seeds is larger, such as position A.

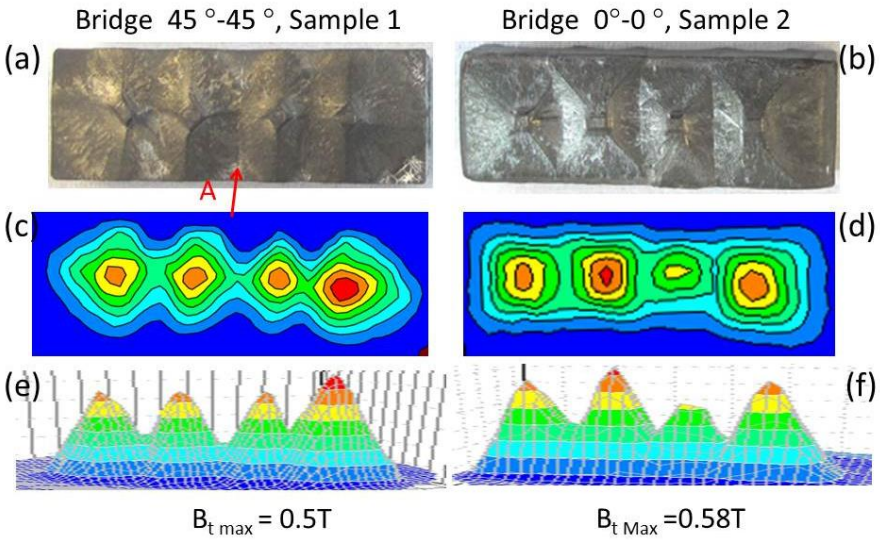

Figure 4. Bridge seeded 0°-0° and 45°-45° YBCO bar-shaped grains and their trapped fields. (a) A photograph of a sample seeded by two 45°-45° bridge seeds, (b) a photograph of a sample seeded by two 0°-0° bridge seeds, (c) and (d) contour maps of the trapped fields of the samples in (a) and (b), (e) and (f) 3D trapped field profiles of the samples in (a) and (b), respectively.

A further example of a multi-seeded, polished YBCO sample of diameter 32 mm with its top surface seeded by a two 45^{o}-45^{o} seeds of 10 mm in length and an inter-seed distance of 7 mm is shown in figures 5(a) and (b). Figures 5(d) and (e) show that closely positioned 45°-45° seeds in the Y direction in figure 5(c) result in a single peak in trapped field, whereas increasing the distance between 45°-45° seeds along the X direction [also in figure 5(c)]

results in the formation of split peaks. This indicates, again, that shorter distance between the seeds decreases the depth of the grain boundary and results in higher trapped fields at positions between the seeds.

Previous research [10, 14-16] suggests that the maximum value of trapped field (with fluctuations) increases when the distance between two seeds decreases for an inter-seed distance of between 2 and 10 mm. The observations presented here extend this earlier research, suggesting further that trapped field decreases with increasing inter-seed distance due to the increased depth of the grain boundary. It is possible, therefore, to conclude that the trapped field profile may exhibit a single peak if the spacing between the pair of bridge seeds is less than approximately 7 mm.

The trapped field profiles in figures 5(d) and (e) were obtained for the full height sample, with a polished, smooth surface in order to allow measurements to be made. The sample was polished further along the *c* direction to remove material from its top surface, which effectively decreases the depth of the grain boundary at its top surface. It can be seen that the trapped field profile for this sample, shown in figures 5(f) and (g), changes to a single, slightly deformed peak, indicating that the grain boundaries are both shallower and are effectively removed by the polishing process. This suggests that there is a significant degree of electrical connectivity in the multi-seeded grain at a distance away from the top surface of the sample, the extent of which is determined by the depth of the grain boundaries and angles of the growth fronts. This evidence for good inter-grain connectivity away from the position of the seeds is further supported by the observation that the trapped field profiles exhibit non-zero values of trapped field between any two seeds. This result is consistent with that reported by Werfel *et al.* in [18], where three seeds were used to seed a bar shaped sample and the trapped field was measured through the sample thickness, leading the authors to conclude that “an additional inter-grain current passing the grain boundaries contributes a substantial part of up to 40% to the measured total trapped magnetic flux density”.

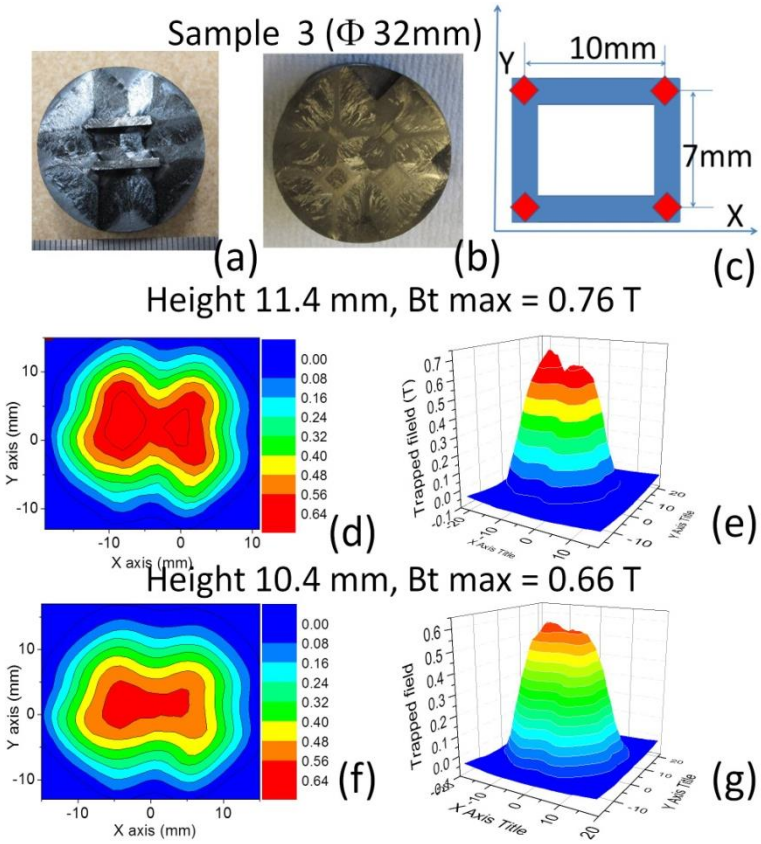

Figure 5. A 45°-45° bridge-seeded YBCO grain and its trapped fields at different thickness. (a) A photograph of a sample seeded by two parallel 45°-45° bridge seeds, (b) a photograph of a polished surface of the sample in (a), (c) a schematic diagram illustrating the arrangement of the two seeds, (d) and (e) trapped field contour map and 3D profile of sample 3 at a height of 11.4 mm, (f) and (g) trapped field contour map and 3D profile of sample 3 at a height of 10.4 mm.

3.3 Effect of the size of the seed and buffer (if buffers are used) together

It can be seen easily from the second and the fourth schematic figures in figure 3 that the depth of the grain boundary is determined primarily by the angle θ between the top surface of the sample and the boundary between the *a* and *c* growth sectors. The angle θ, in turn, is determined by the single grain growth rate and is therefore constant for constant growth parameters. As a result, the only way to decrease the height of the grain boundary is to reduce the distance between the seeds if these parameters remain fixed for a given TSMG growth process. However, buffer pellets can be employed to effectively enlarge the seeded area on the surface of the sample [28]. Sample 4, for example, is a bar shaped YBCO sample that was grown using 3 buffer pellets [25-27] and SmBCO seeds separated by 20 mm (centre to centre) and aligned in a 0°-0°-0° configuration. Each buffer pellet was 7 mm in diameter and 1 mm

in thickness after melt growth. It can be seen from figure 5 that the maximum field of sample 4 and the depth of the troughs in trapped field are similar to that of sample 2, even though the seeds are further apart (20 mm). This is because the effective length *L* between the seeds due to the inclusion of the buffer layers is reduced, which suggests that the buffer technique can be used to decrease the effective length of the seeds so that the depth of the grain boundary decreases compared to samples melt processed without buffers.

A sample with relatively extensive growth along the *c*-direction is desirable given that its top surface will inevitably contain grain boundaries. The use of a buffer pellet is equivalent to introducing a complete additional layer of YBCO during the growth process to effectively increase the height and extent of growth along the *c*-direction, and, hence, it is therefore more economical to use a series of small buffers. Modelling indicates that the optimum aspect ratio between the radius and height of a cylindrical sample is 1: 1.3 for a YBCO single grain sample to exhibit a uniform J_c [29]. The seeding of multi-seeded samples can also be designed to yield the optimum or desired trapped field distribution. However, J_c is not uniform and the value of θ will vary with different precursor powder composition, heat profile, growth atmosphere and furnace used. Therefore, the best process design for the growth of multi-seeded samples may vary in different institutions based on the detailed parameters employed locally for sample growth. It should be noted further that relative variations in the vertical length of the grain boundary and the height of the parent grain and the seed separation distance are also related critically to the size of the sample.

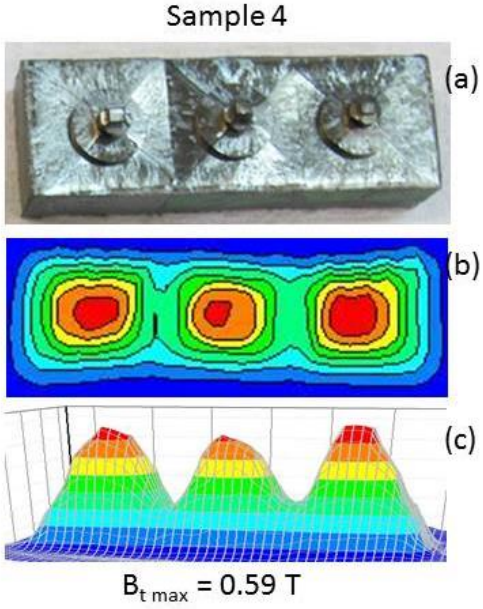

Figure 6. A 0°-0°-0° seeded YBCO bar-shaped sample and its trapped fields profiles at 77 K. (a) A photograph of a bar shaped YBCO sample seeded using 3 seeds and associated buffer layers, (b) the trapped field contour map of the sample in (a) and (c) 3D trapped field profile of the sample in (a).

Sample 5, shown in figure 6, was fabricated to investigate this effect further by using two SmBCO seeds separated by 14 mm, but with two buffer layer stack. In this case, the buffer layer immediately beneath the seed was of diameter of 4 mm, and that between this buffer layer and the top surface of the sample of diameter 7 mm, corresponding to a total stacked buffer layer height of 2 mm. The SmBCO seeds were cut into rectangular shapes with an aspect ratio of 2:3 to simplify their alignment. The distance between the nearest edges of the lower buffer layers in this arrangement was only 1 mm. The sample was polished sequentially through its *c* axis and the trapped fields were measured successively at each height. Each trapped field was measured at 77 K by a rotating array of 18 Hall probes positioned 1.0 mm above the top surface of the sample. The maximum value of trapped field was calibrated by a hand-held probe located at the top surface, with the sensor located 0.5 mm away from the sample surface.

Figures 7(d) and (e) indicate that there is one peak in the trapped field profile measured at the top surface when measured at the full sample height of 11.4 mm. Figure 7(f) shows that there are actually two peaks in this field distribution with a shallow trough, measured using a hand probe against the top surface, with a maximum trapped field value is 0.54 T. At a sample height of 10.8 mm, figures 7(h) and (i), show that there is one peak in the trapped field profile measured at the top surface, with figure 7(j) indicating that the trough is so shallow that there is actually no clear discontinuity in slope in the trapped field profile when the hand probe is used, and a maximum trapped field of 0.58 T. When the height of the sample is further reduced to 10.3 mm, it can be seen from figures 7(l) and (m) that there is an ever-increasing trend toward a single peak in the tapped field profile measured from the top surface using the array of probes. Figure 7(n) reveals further that the field profile measured by the hand-held probe exhibits a plateau, and an even higher maximum trapped field of 0.61 T. These results suggest that increasing the size of the effective seeding area of the sample by utilising buffers that act as seeds [28], and therefore decreasing the length between the seeds, can decrease the depth of the grain boundary very effectively. The trapped field can increase without extensive polishing along the *c*-direction of the sample, suggesting that the grain boundary depth

becomes negligible and that the sample remaining after polishing effectively constitutes a single grain.

Inhomogeneities within the bulk superconductor affect the dynamics of the flux entering the sample, causing a distortion in the trapped field profile, with flux being trapped preferentially in regions of stronger pinning (higher J_c). The effectiveness of the Pulse Magnetisation process is affected significantly by the uniformity of the grain being magnetised, which, in turn, leads to the localised generation of heat via induced eddy currents [30, 31]. As such, the effect on the Pulse Magnetisation process of a multi-seeded sample containing grain boundaries should generate some interesting results. The Pulse Magnetisation process was applied to sample 5 for a height of 11.4 mm. A pulsed magnetic field was applied 5 times at 77 K using sequential peak values of 0.35, 0.7, 1.4, 2.1 and 2.8 T, and a hand probe used to measure the trapped field values at the surface of the sample after every pulse along the line between the two seeds. The distance between the probe (which is located inside the measuring tube) and surface of the sample was estimated to be 0.5 mm. Figure 7(b) shows the results of the trapped field measurements. It can be seen that the threshold applied field for the magnetisation of sample 5 is around 0.7 T (which means the magnetic flux has penetrated to the centre of the sample [31]) and saturates at 0.54 T (which means the sample has trapped a maximum amount of flux) when the applied field was 2.1 T.

It can be seen that sample 5 exhibits two peaks in the trapped field profile when measured more precisely, although the trough is not deep. The top surface of sample 5 was polished from the stage shown in figure 7(k) and the grain boundary between the two seeds examined using an optical microscope at a magnification of ×50. Figure 8(a) shows that the grain boundary of this sample after polishing away 1.0 mm from the top surface is very thin and discontinuous. Cutting sample 5 subsequently through the vertical plane intersecting the two seeds to the bottom of the sample enabled the same grain boundary to be observed through the sample cross-section. Figure 8(b) shows that the grain boundary is shallow, being only about 1 mm deep, which indicates that it is not a prominent feature of the sample microstructure. All these results suggest that, with careful design of the size of the seed and length between seeds corresponding to a certain sample size, it is possible to fabricate grains with a shallow grain boundary (i.e. quasi-single grains). The buffer layers used in this case help to increase the effective size of the seeds.

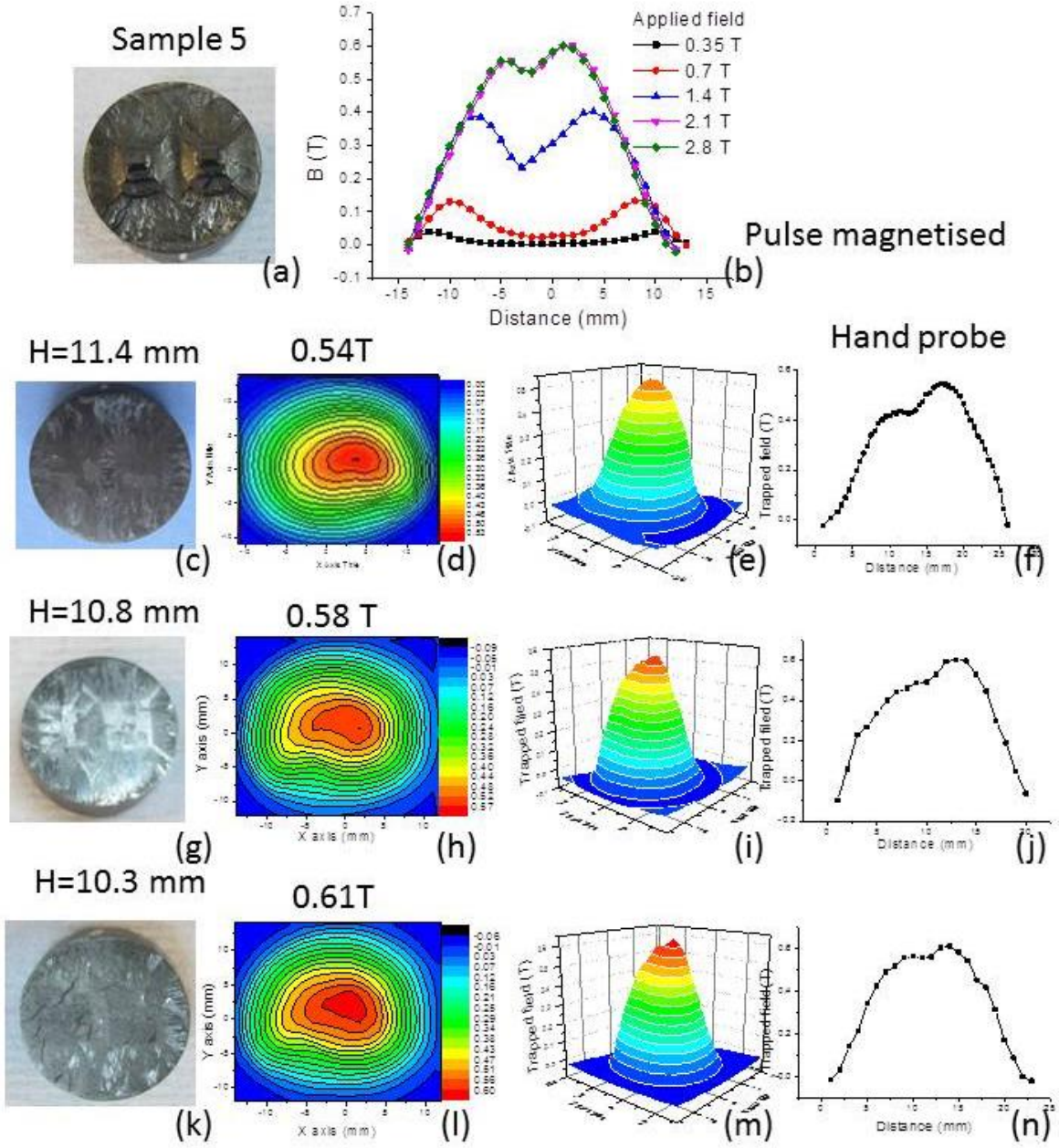

Figure 7. The trapped fields measured by Pulse-Magnetisation for a buffer aided 0°-0° YBCO single grain (sample 5) for different sample heights measured by Field-Cooling. (a) A photograph of the multi-seeded YBCO sample 5, (b) the trapped fields obtained by Pulse Magnetisation at 0.35, 0.7, 1.4, 2.1 and 2.8 T, (c) a photograph of a polished surface of sample 5 at a height of 11.4 mm, (d) and (e) trapped fields contour map and corresponding 3D profile measured by a rotating array of 18 probes, (f) trapped field measured in one direction by a hand probe at a distance 0.5 mm from the top surface of the sample, (g) a photograph of a polished surface of sample 5 at height 10.8 mm, (h) and (i) trapped field contour map and corresponding 3D profile of sample 5 at a height of height 10.8 mm

measured by a rotating array of 18 probes, (f) trapped field of sample 5 at a height of 10.8 mm measured in one direction, (k) a photograph of a polished surface of sample 5 at a height of 10.3 mm, (l) and (m) trapped field contour map and corresponding 3D profile of sample 5 at a height of 10.3 mm measured by a rotating array of 18 probes, (f) trapped field of sample 5 at a height of 10.3 mm measured in one direction.

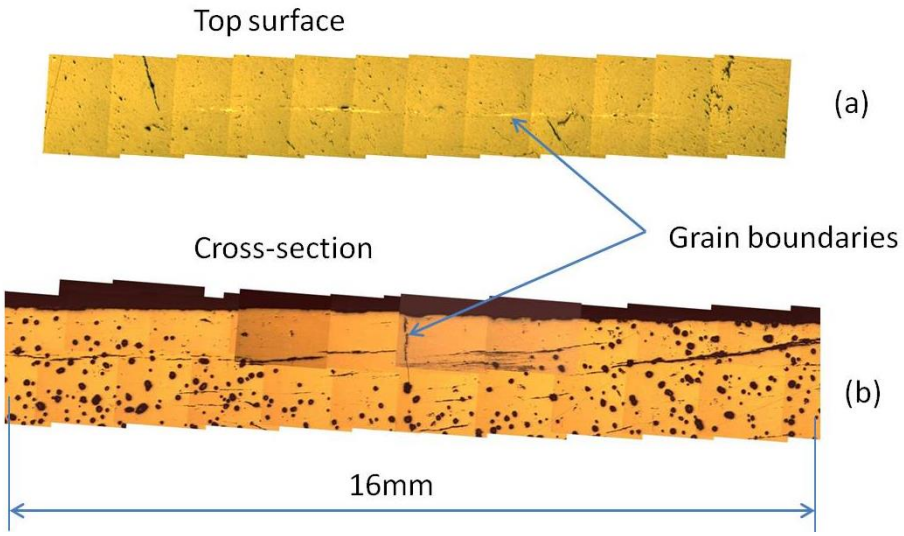

Figure 8. Microstruces of the grain boundaries of sample 5 at a magnification of x50. (a) The grain boundary at the top surface intermediate between the two seeds (the grain boundary is papendicular to the line connecting the two seeds). (b) The grain boundary in the sample cross-section that cuts through the two seeds.

3.4 Effect of the alignment of the seed and buffer (if buffers are used) together

The above conclusions of the influence of the size of the seeds and inter-seed distance on the properties of the grain boundary are only true if the seeds are aligned well. Even a clean grain boundary between misaligned individual grains could inhibit seriously the flow of the supercurrent, and especially when the angle between the two grains is larger than 10° [17, 32, 33]. In consequence, the resulting trapped field in a multi-seeded sample is dependent critically on the relative orientation of the seeds. In order to achieve the best possible alignment of the two seeds, therefore, rectangular shaped SmBCO seeds with a specific aspect ratio of 3:2 were used to grow sample 5 to enable the effect of seed alignment to be investigated. Thin film seeds [24] with the same aspect ratio (3:2) were also used to fabricate sample 6, which was a GdBCO-Ag sample of diameter 20 mm and height 9 mm, as shown in figure 9(a). Figures 9(b) and (c) show a contour map and three-dimension profile of the

trapped field measured by the rotating array of 18 Hall probes, respectively. It can be seen that the trapped field of sample 6 exhibits one, rather broad peak when the probes are 1 mm away from the polished sample surface. The trapped field measured by the hand-held probe along the top surface of sample 6 shows two peaks, although the trough is shallow and the trapped field value is as high as 0.8 T [figure 9(d)]. The trapped fields [figure 9(g)] obtained using Pulse Magnetisation provide further confirmation that the trough between the two peaks of sample 6 is shallow. Interestingly, the activation field of this sample is less than 0.7 T, although the largest trapped field can be as high as 0.8 T at the top surface of the sample. This suggests that, compared to the 0°-0° seeded YBCO sample 5, it is easier for magnetic flux to penetrate the 0°-0° seeded GdBCO-Ag sample 6 but more difficult for the flux to move out of the sample, which is a desirable property for the application of multi-seeded bulk superconductors. Pulse Magnetisation provides a good diagnostic tool for investigating the field trapping properties and other information for understanding the properties of multi-seeded bulk superconductors.

Importantly, the trapped field at the bottom of the sample was also measured and is presented in figures 9(e) and (f). It can be seen that the peak of the trapped field is sharper and exhibits a more circular cross-section and the distribution of the trapped field is more uniform, indicating that sample 6 is effectively a single grain towards the bottom and the grain boundary at the top of the sample is so shallow that it does not influence the trapped field profile at the bottom of the sample. In other words, carefully designed and grown multi-seeded bulk (RE)BCO superconducting samples can constitute quasi-single grains with a shallow grain boundary close to the top surface with the rest of the sample behaving as a single grain. This property is especially beneficial for developing multi-seeded bulk superconductors for large-scale applications.

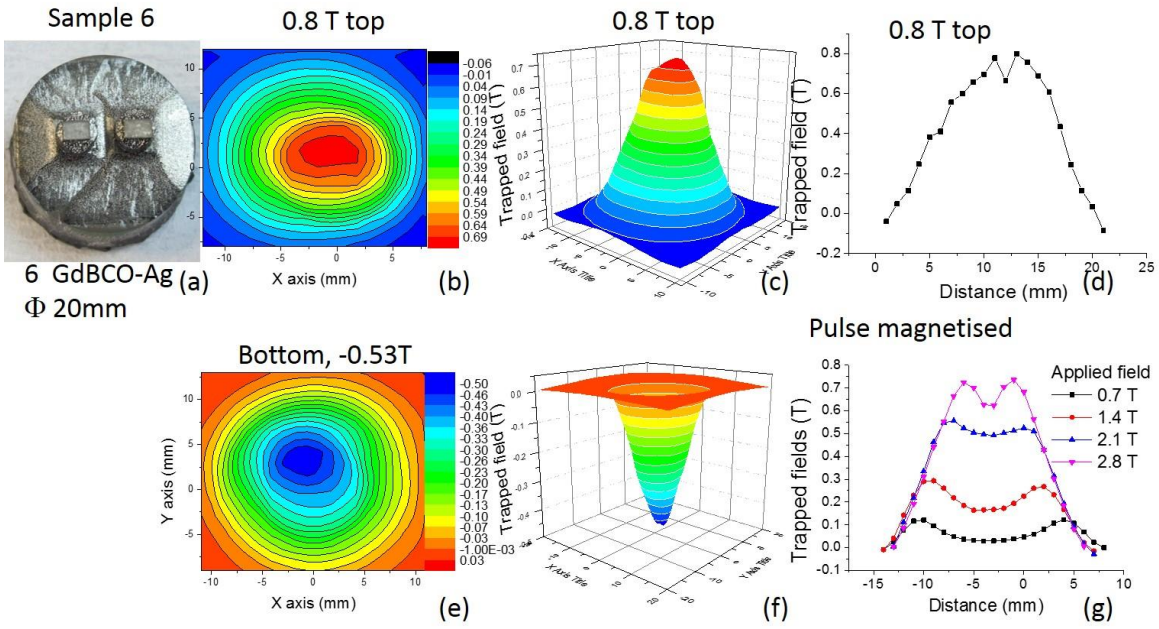

Figure 9. A buffer aided 0°-0° GdBCO-Ag single grain and its trapped fields generated by zero-field cooling and Pulse-Magnetisation. (a) A photograph of a GdBCO-Ag sample seeded by two, thin film seeds, (b) and (c) trapped field contour map and 3D profile of sample 6 at the polished top surface measured by a rotating array of 18 probes, (d) trapped field of sample 6 at the top surface along one direction measured by the hand-held probe at a distance 0.5 mm away from the surface of the sample, (e) and (f) trapped field contour map and 3D profiles of sample 6 at the polished bottom surface measured by a rotating array of 18 probes and (g) trapped fields obtained by pulse magnetisation at 0.7, 1.4, 2.1 and 2.8 T, respectively.

4 Conclusions

We have demonstrated that multi-seeded quasi-single grains can be fabricated by top seeded melt growth with careful control of the distance between the seeds, the size of the seeds (and buffer layers) and, most importantly, the alignment of the seeds. The effect of grain boundaries in multi-seeded samples can be reduced by decreasing the distance between seeds and by increasing the size of the seeds (or buffer layers), providing the seeds are fully aligned, and particularly with the aid of bridge-shaped seeds or seeds with a tailored aspect ratio. As a result, multi-seeding can be used to fabricate high quality quasi-single grains, with a minimum grain boundary region at the top surface of the sample where the seeds are located, and without any evidence of a grain boundary at the bottom surface of the multi-seeded grain.

Acknowledgement

We acknowledge the Engineering and Physical Sciences Research Council (EPSRC grant ref. EP/K02910X/1) for financial support. Additional data related to this publication are available at the University of Cambridge data repository
https://www.repository.cam.ac.uk/handle/1810/255872

References

[1] Hull, J. R.; Murakami, M. *Proceedings of the IEEE* **2004**, *92*. 1705-1718.

[2] John, R. H. *Superconductor Science and Technology* **2000**, *13* p. R1.

[3] Durrell, J. H.; Dennis, A. R.; Jaroszynski, J.; Ainslie, M. D.; Palmer, K. G. B.; Shi, Y. H.; Campbell, A. M.; Hull, J.; Strasik, M.; Hellstrom, E. E.; Cardwell, D. A. *Superconductor Science and Technology* **2014**, *27* p. 082001.

[4] Endo, A.; Chauhan, H. S.; Nakamura, Y.; Shiohara, Y. *Journal of Materials Research* **1996**, *11*. 1114-1119.

[5] Shi, Y. H.; Yoeh, W.; Dennis, A. R.; Babu, N. H.; Pathak, S.; Xu, Z.; Cardwell, D. A. *Journal of Physics: Conference Series* **2010**, *234* p. 012039.

[6] Shi, Y.; Hasan, T.; Babu, N. H.; Torrisi, F.; Milana, S.; Ferrari, A. C.; Cardwell, D. A. *ACS Nano* **2012**, *6*. 5395-5403.

[7] Nariki, S.; Sakai, N.; Murakami, M.; Hirabayashi, I. *Physica C: Superconductivity* **2004**, *412–414, Part 1*. 557-565.

[8] Kim, C.-J.; Hong, G.-W.; Oh, H.-J. *Physica C: Superconductivity* **2001**, *357–360, Part 1*. 635-641.

[9] Kim, C.-J.; Kim, H.-J.; Jee, Y. A.; Hong, G.-W.; Joo, J.-H.; Han, S.-C.; Han, Y.-H.; Sung, T.-H.; Kim, S.-J. *Physica C: Superconductivity* **2000**, *338*. 205-212.

[10] Kim, C.-J.; Kim, H.-J.; Joo, J.-H.; Hong, G.-W.; Han, S.-C.; Han, Y.-H.; Sung, T.-H.; Kim, S.-J. *Physica C: Superconductivity* **2000**, *336*. 233-238.

[11] Haindl, S.; Eisterer, M.; Weber, H. W.; Babu, N. H.; Cardwell, D. A. *Applied Superconductivity, IEEE Transactions on* **2005**, *15*. 3129-3132.

[12] Withnell, T. D.; Babu, N. H.; Iida, K.; Shi, Y.; Cardwell, D. A.; Haindl, S.; Hengstberger, F.; Weber, H. W. *Physica C: Superconductivity and its Applications* **2006**, *445–448*. 382-386.

[13] Cheng, L.; Guo, L. S.; Wu, Y. S.; Yao, X.; Cardwell, D. A. *Journal of Crystal Growth* **2013**, *366*. 1-7.

[14] Shi, Y. H.; Durrell, J. H.; Dennis, A. R.; Babu, N. H.; Mancini, C. E.; Cardwell, D. A. *Superconductor Science and Technology* **2012**, *25* p. 045006.

[15] Shi, Y. H.; Durrell, J. H.; Dennis, A. R.; Cardwell, D. A. *Superconductor Science and Technology* **2013**, *26* p. 015012.

[16] Shi, Y.; Durrell, J. H.; Dennis, A. R.; Zhang, Z.; Zhai, W.; Hari Babu, N.; Cardwell, D. A. *Journal of the American Ceramic Society* **2013**, *96*. 1757-1762.

[17] Durrell, J. H.; Rutter, N. A. *Superconductor Science and Technology* **2009**, *22* p. 013001.

[18] Werfel, F. N.; Floegel-Delor, U.; Riedel, T.; Goebel, B.; Rothfeld, R.; Schirrmeister, P.; Wippich, D. *Physica C: Superconductivity* **2013**, *484*. 6-11.

[19] Deng, Z.; Miki, M.; Felder, B.; Tsuzuki, K.; Shinohara, N.; Hara, S.; Uetake, T.; Izumi, M. *Physica C: Superconductivity* **2011**, *471*. 504-508.

[20] Wongsatanawarid, A.; Seki, H.; Murakami, M. *Journal of Physics: Conference Series* **2010**, *234* p. 012047.

[21] Choi, J. S.; Park, S. D.; Jun, B. H.; Han, Y. H.; Jeong, N. H.; Kim, B. G.; Sohn, J. M.; Kim, C. J. *Physica C: Superconductivity* **2008**, *468*. 1473-1476.

[22] Sawamura, M.; Morita, M.; Hirano, H. *Superconductor Science and Technology* **2004**, *17* p. S418.

[23] Sawamura, M.; Morita, M.; Hirano, H. *Physica C: Superconductivity* **2003**, *392–396, Part 1*. 441-445.

[24] Chen, Y.; Cui, X.; Yao, X. *Progress in Materials Science* **2015**, *68*. 97-159.

[25] Shi, Y. H.; Dennis, A. R.; Cardwell, D. A. *Superconductor Science and Technology* **2015**, *28* p. 035014.

[26] Devendra Kumar, N.; Shi, Y.; Zhai, W.; Dennis, A. R.; Durrell, J. H.; Cardwell, D. A. *Crystal Growth & Design* **2015**, *15*. 1472-1480.

[27] Zhao, W.; Yunhua, S.; Dennis, A. R.; Cardwell, D. A. *Applied Superconductivity, IEEE Transactions on* **2015**, *25*. 1-5.

[28] Yunhua, S.; Devendra Kumar, N.; Wen, Z.; John, H. D.; Anthony, R. D.; David, A. C. *Superconductor Science and Technology* **2016**, *29* p. 015010.

[29] Eisterer, M.; Haindl, S.; Zehetmayer, M.; Gonzalez-Arrabal, R.; Weber, H. W.; Litzkendorf, D.; Zeisberger, M.; Habisreuther, T.; Gawalek, W.; Shlyk, L.; Krabbes, G. *Superconductor Science and Technology* **2006**, *19* p. S530.

[30] Ainslie, M. D.; Zou, J.; Mochizuki, H.; Fujishiro, H.; Shi, Y. H.; Dennis, A. R.; Cardwell, D. A. *Superconductor Science and Technology* **2015**, *28* p. 125002.

[31] Ainslie, M. D.; Fujishiro, H.; Ujiie, T.; Zou, J.; Dennis, A. R.; Shi, Y. H.; Cardwell, D. A. *Superconductor Science and Technology* **2014**, *27* p. 065008.

[32] Todt, V. R.; Zhang, X. F.; Miller, D. J.; St. Louis-Weber, M.; Dravid, V. P. *Applied Physics Letters* **1996**, *69*. 3746-3748.

[33] Ch, J.; Bringmann, B.; Delamare, M. P.; Walter, H.; Leenders, A.; Freyhardt, H. C. *Superconductor Science and Technology* **2001**, *14* p. 260.

For table of contents only

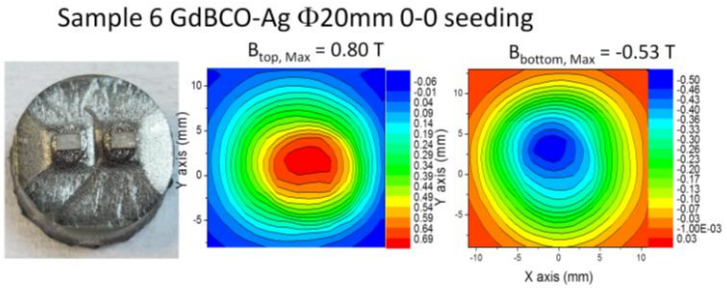

TOC: A multi-seeded 0°-0° GdBCO-Ag single grain and its trapped field profiles which indicate that sample 6 is a single grain from the measurements at both top and bottom surfaces.